sustainability

MDPI

Article

Reliability and Robustness Assessment of Highway Networks under Multi-Hazard Scenarios: A Case Study in Xinjiang, China

Weihua Zhu [1,2], Shoudong Wang [1,2,*], Shengli Liu [1,2], Xueying Gao [1,2], Pengchong Zhang [1,2] and Lixiao Zhang [3]

1 Transport Planning and Research Institute, Ministry of Transport, Beijing 100028, China
2 Laboratory of Transport Safety and Emergency Technology, Beijing 100028, China
3 State Key Joint Laboratory of Environmental Simulation and Pollution Control, School of Environment, Beijing Normal University, Beijing 100875, China
* Correspondence: wangsd@tpri.org.cn

Abstract: The robustness and reliability capacities of highways are particularly critical when dealing with emergencies in order to ensure user safety following disaster events. Assessing the robustness and reliability of highways under multi-hazard scenarios and evaluating the impact of planning on them have become urgent topics. In this study, we use the Xinjiang Production and Construction Corps' (XPCC) existing and planned arterial highway networks in China for research. Based on the multi-hazard information, we established and employed four attack strategies on the existing and planned arterial highway networks. The results show that the exposure susceptibility coefficient (ESC) strategy has a higher destruction capability than the random attack strategy, which is close to the greedy algorithm coefficient (GAC) strategy. In addition, attacks have negligible impacts on connectivity reliability and robustness but significantly affect travel time reliability and robustness. When the number of removed edges reaches 20 using the ESC strategy, the travel time reliability drops to 0.4 for the existing highway network. In addition, the planned highway network significantly improves the reliability and robustness with regard to multi-hazard scenarios, especially for travel time reliability. Travel time reliability is improved by 10% under the historical damage records coefficient (HDRC) and ESC attacks. Our study shows that planning promotes the construction of a resilient transportation system in multi-hazard scenarios, providing valuable information for resilient transportation construction.

Keywords: robustness assessment; reliability assessment; multi-hazards; exposure assessment; Xinjiang Production and Construction Corps

check for updates

Citation: Zhu, W.; Wang, S.; Liu, S.; Gao, X.; Zhang, P.; Zhang, L. Reliability and Robustness Assessment of Highway Networks under Multi-Hazard Scenarios: A Case Study in Xinjiang, China. *Sustainability* **2023**, *15*, 5379. https://doi.org/10.3390/su15065379

Academic Editors: Golam Kabir, Muntasir Billah and Subhrajit Dutta

Received: 7 February 2023
Revised: 9 March 2023
Accepted: 16 March 2023
Published: 17 March 2023

1. Introduction

The transportation network is a critical element of economic and societal activities, as it serves as the foundation for the transfer of goods and the movement of people. However, natural hazards may damage or disrupt transportation systems, especially in disaster-prone areas. Roads and other exposed areas, such as factories and communities, will be the first to be directly damaged when natural disasters occur. In addition, the uncertain connectivity and longer travel times for transportation will significantly extend the impact on general well-being and the economy [1,2], as shown in Figure 1. In February 2021, heavy rainfall and melting snow caused some banks of the Rhine River, Europe's most important commercial waterway, to burst, triggering a halt in shipping via the river for several days, which disrupted the flow of both inbound raw materials and outbound product delivery [3]. In the 2008 Wenchuan earthquake, all of the highways in Wenchuan (and others throughout Sichuan province) were damaged, causing a delay in rescue activities, which resulted in more severe casualties [4]. In order to support the economic system and the construction of a modernized socialist country, the Chinese government has complied with a plan and built a modern high-quality and reliable national transportation network with high robustness [5]. In this context, assessing the robustness and reliability of transportation networks under multi-hazard scenarios and evaluating the impact of planning on network resilience has become an urgent topic.

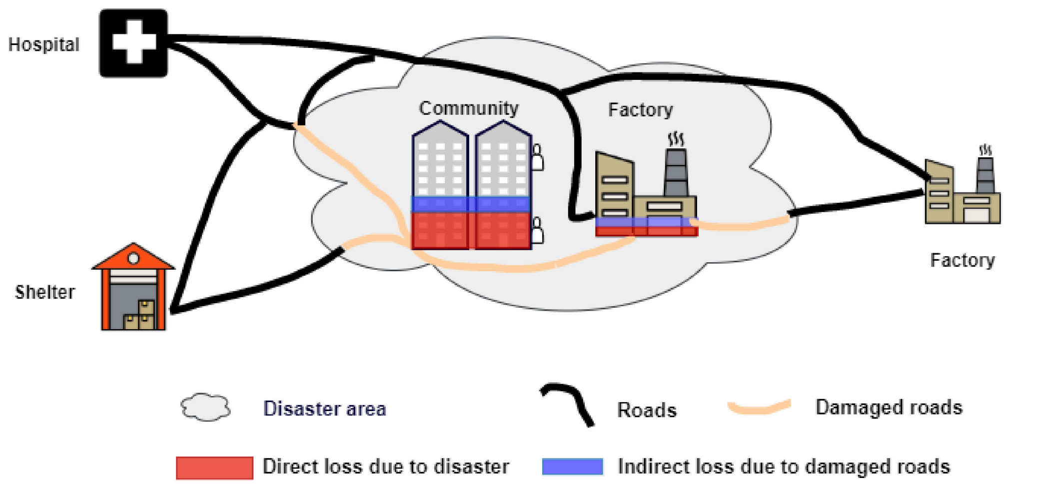

Figure 1. Impacts due to natural hazards and damaged roads. In the disaster area (grey), the community and factory will be affected immediately when the disaster occurs (red presents direct loss for the community and factory due to a disaster). After the disaster, indirect losses may occur since aggravated injury due to untimely rescue and supply to the disaster area is hampered (blue is the indirect loss for the community and factory due to damaged roads).

Recently, many studies have focused on the resilience of transportation systems [6–8]. In general, a resilient transportation network has the capacity for high reliability, strong robustness, rapid recovery, etc., to cope with bad scenarios. Among them, reliability and robustness are described as an ability to cope with a situation when an accident occurs. The reliability of a transportation system [9–12] is usually defined as the probability that a system can perform its desired function to an acceptable level of performance for a given period or under special conditions. Studies on reliability generally focus on three concepts: connectivity reliability [13,14], travel time reliability [9,12,15–17] and capacity reliability [15]. Jiang and Huang [14] analyzed connectivity reliability for highway networks in high-intensity seismic regions using the Bayesian network. Leng et al. [15] evaluated the travel time reliability and capacity of an urban road network under icy and snowfall conditions. Network robustness [18,19] is commonly defined as the capability of a network to maintain functionality (or connectivity) when a sequential component removal strategy is performed. Several studies [18,20] recently investigated the robustness of transportation systems under different attack strategies by considering defense and potential alternatives combined with actual situations. Zhu et al. [20] assessed the robustness of the Shanghai and Beijing metro networks using strategic defense. De-Los-Santos et al. [18] evaluated passenger robustness in a rail transit network considering alternative transportation modes. However, few studies focus on reliability and robustness under multi-hazard scenarios, particularly on the changes between the existing and planned road networks.

To bridge these gaps, this study aims to assess the reliability and robustness of highway networks based on multi-hazard scenarios. The existing and planned highway networks in Xinjiang Production and Construction Corps (XPCC) and highway damage records due to geological events, earthquakes and floods, as well as multi-hazard distribution information, are used. We first generate reliability and robustness metrics from time and connectivity dimensions. Based on the multi-hazard information and the designed targeted strategies, we analyze the reliability and robustness of the highway network using four attack approaches. We also investigate how planned roads influence the reliability and robustness of the highway network. The remainder of the article is organized as follows:

Section 2 describes the data, including the highway data, natural hazards and historical highway damaged data. In Section 3, we introduce the method for evaluating the reliability and robustness of highway networks, including multi-hazard exposure assessments, the metrics definition, and attack strategy design. Section 4 presents the main findings and results. Sections 5 and 6 provide the discussion and conclusion, respectively, of this article.

2. Data

The Xinjiang Production and Construction Corps (XPCC) highway network is used as a case study to assess its reliability and robustness under multi-hazard scenarios. The highway built by the XPCC plays a vital role in society and the economy by carrying out an essential mission of China's strategic layout for growth [21]. By the end of 2021, the XPCC highway mileage reached 38,014 km. In 2021, the XPCC had served 9.92 million passengers and carried 139.10 million tons of commercial freight [22]. However, the XPCC highway's exposure to multi-hazards varies significantly due to the different disaster-prone regions it covers. In recent years, floods and geological disasters have repeatedly occurred on the XPCC highway, causing transportation disruptions and economic losses. For example, in the past ten years, there have been ten flood events at K17+452 of the Shibo Line and six debris flow events at K17+960 of the Wukong Line in XPCC [23].

2.1. Highway Data

In this study, we obtained the highway infrastructure information from the transportation bureau of the XPCC to assess the multi-hazard exposure, as shown in Figure 2a. Here, we define multi-hazard exposure as the value or the length of assets subject to the multi-hazards [24]. In addition, we generated the existing and planned (the planning period is from 2021 to 2050) arterial highway networks of the XPCC to assess the highway reliability and robustness, as shown in Figure 2b [25]. The topological network was defined using the space L method [26]. The space L network topology uses nodes representing road crossings and edges representing road lines between two consecutive sites.

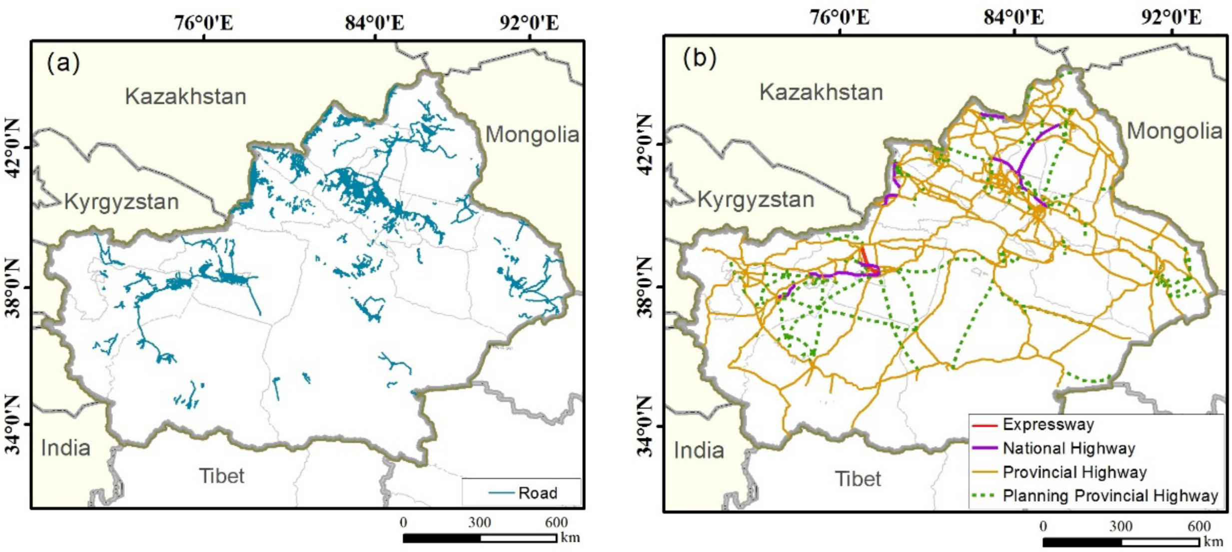

Figure 2. (**a**) Highway infrastructure of the XPCC and (**b**) the existing and planned arterial highway networks of the XPCC.

2.2. Natural Hazards

Geological hazards, floods, earthquakes and snow are the four major natural hazards faced by the XPCC highways [23]. As the XPCC does not have highway damage records concerning snow, we only selected geological disasters, floods, and earthquakes for our analysis.

Geological hazards: The geological hazard data used in this study were collected by the Institute of Geographic Sciences and Natural Resources Research at the Chinese Academy of Sciences [27]. In this dataset, the geological point data are expressed as the point, which includes several geological types, such as landslides, debris flows, ground fissures, land subsidence, landslides, and slopes.

Flood hazard map: GLOFRIS global fluvial flood hazard maps were used as flood hazard data in this study, which are developed using the GLOFRIS modelling cascade provided by Ward et al. [28] and Winsemius et al. [29]. The flood design standard for Chinese highways was designed for a 100-year water depth, according to the standard for flood control [30]. In this study, a 100-year return period flood map was used to estimate flood exposure. The resolution of the flood map is 30 arcsec (ca. 1 km.).

Seismic hazard map: A seismic hazard map was obtained from the GB18306—2015 "Seismic ground motion parameter zonation map of China" [31], which shows the peak ground acceleration with a 10% probability of exceedance in 50 years. In China, the specifications for the seismic design of highway subgrades, bridges, and tunnels are based on GB18306—2015 [31].

2.3. Historical Highway Damage Data

We catalogued 172 damaged road records, including damage locations, damage types, and the number of damage times from 2011 to 2021 caused by the geological hazards, earthquakes, and floods on XPCC roads [23]. The spatial distribution of road damage data is presented in Figure 3. The results show that the XPCC roads suffered widespread damage, particularly in areas 5, 3, and 8, which account for 23.26%, 18.02%, and 11.63% of the total, respectively. Among the 172 damaged road records, 128 were caused by floods, accounting for 74.42%, and 17 were caused by landslides, accounting for 9.88%. In addition, 51 damaged road records are located on the main highway.

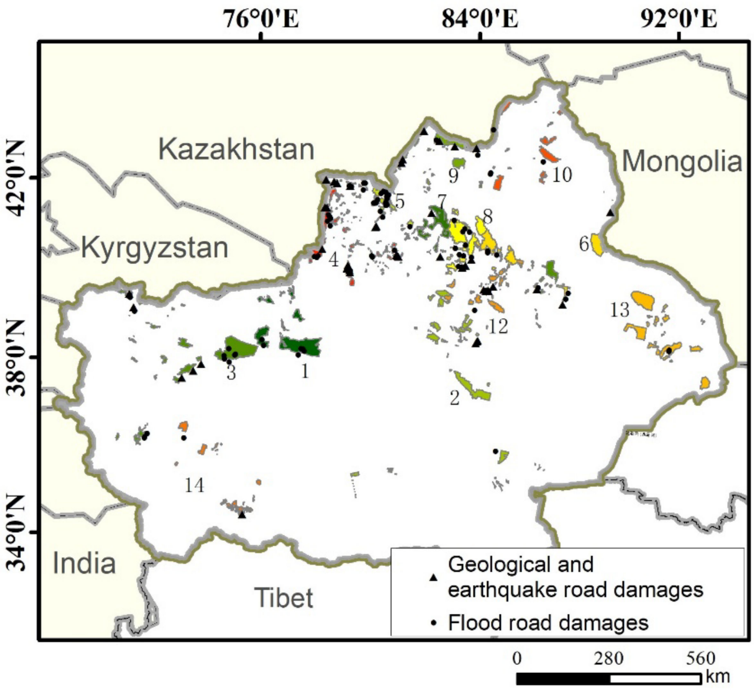

Figure 3. Spatial distribution of historical data on damaged roads from 2011 to 2021.

3. Method

3.1. Exposure Assessment

Geological hazards: The exposure analysis of XPCC highways under geological hazards is based on the number of geological hazard points. The highway lines were split into

5 km sections. Along both sides of the sections, we generated affected 5 km buffers. Then, we determined the number of geological hazard points within the affected buffer as the affected geological hazards. Exposure susceptibility is grouped into five classes according to the number of geological hazard points: <2 (very low), 2–5 (low), 5–10 (medium), 10–100 (high), and ≥100 (very high) [32].

Seismic hazard map: The seismic exposure analysis of the XPCC highway is the peak ground acceleration with a 10% probability of exceedance in 50 years, which was obtained by overlaying the highway line on the seismic map. Exposure susceptibility is grouped into five classes according to the PGA: ≤0.1 g (very low), 0.1–0.15 g (low), 0.15–0.2 g (medium), 0.2–0.3 g (high), and >0.3 g (very high) [32].

Flood hazard map: The flood exposure analysis of the XPCC highway is based on the 100-year return period flood map, which was obtained by overlaying the highway line on the flood map. Exposure susceptibility is grouped into five classes according to the flood depth: <0.1 m (very low), 0.1–0.2 m (low), 0.2–0.4 m (medium), 0.4–0.8 m (high), and 0.8–1.8 m (very high) [32].

3.2. Reliability and Robustness Assessment

3.2.1. Reliability and Robustness Connectivity Metric

An independent path between two nodes (the two paths do not share any nodes except the start and end points) is called the connectivity between two nodes [33]. We defined the highway network connectivity reliability (C_Rel) as the probability of more than one independent path between two nodes in the highway network after an accident has occurred, which is calculated by:

$$C\_Rel = P(C_{st} \geq 1)\ (s, t \in N,\ \ s \neq t) \tag{1}$$

where N is the number of the node of the highway and C_{st} is the connectivity between node s and node t.

In addition, we defined the road network connectivity robustness (C_Rob) as the ratio of the total connectivity after and before an accident, which is calculated by Equation (2):

$$C\_Rob = \frac{C^{-ij}}{C}\ (s \neq t) \tag{2}$$

where C and C^{-ij} are the highway network connectivity before and after some component failures. The highway network connectivity is calculated by Equation (3):

$$C = \sum\nolimits_{s,t}^{N} C_{st}\ (s \neq t) \tag{3}$$

3.2.2. Reliability and Robustness Travel Time Metric

In this study, we defined the highway network travel time reliability (T_Rel) as the probability that the travel time exceeds 10% [34] between two nodes in the road network after an accident has occurred, which is calculated by:

$$T\_Rel = P\left(\frac{T_{st}^{-ij} - T_{st}}{T_{st}} > 0.1\right)\ (s, t \in N,\ s \neq t) \tag{4}$$

where T_{st} is the time of the shortest path between nodes s and t, while the nodes cannot reach each other, $T_{st} = \infty$, which is calculated by the length and speed of the shortest path. The speed of the expressway is 120 km/h and 80 km/h for national highways and provincial highways, respectively [30].

In addition, we defined the highway network travel time robustness (T_Rob) based on the network efficiency, which is calculated by the ratio of the network efficiency after and before an accident, which is calculated by Equation (5):

$$T\_Rob = \frac{E^{-ij}}{E} \ (s \neq t) \tag{5}$$

where E and E^{-ij} are the road network efficiency before and after some component failures. The road network efficiency is calculated by Equation (6):

$$E = \sum_s \sum_t \frac{1}{T_{st}} (s \neq t) \tag{6}$$

3.2.3. Attack Strategies Definition

In this framework, we considered two types of attacks, a random attack and a targeted attack. The random attack occurs when the attacked node is randomly selected from all nodes of the network with equal probability. Meanwhile, the targeted attack sequentially removes the nodes according to the important criteria defined by the attacker's strategy. In this study, we investigated the reliability and robustness of current and planned highway networks by employing attack models. We examined three targeted strategies for identifying influential nodes, as described below.

3.2.4. Historical Damage Records Coefficient

The historical damage records coefficient (HDRC) describes the number of damage records to an edge. The HDRC of edge ij is defined as follows:

$$H_{ij} = \frac{D_{ij}}{D} \ (s \neq t) \tag{7}$$

where D is the number of historical damage records for the highway network and D_{ij} is the number of historical damage records affected edge ij. An edge with a higher HDRC is an edge easily affected by hazards. The HDRC strategy sequentially removes the edges in descending order based on the HDRC. If multiple edges have the same highest HDRC, one of these edges is randomly chosen.

3.2.5. Exposure Susceptibility Coefficient

The exposure susceptibility coefficient (ESC) is defined based on the multi-hazard exposure susceptibility score, which is calculated as follows:

$$E_{ij} = \frac{g_{ij} + f_{ij} + e_{ij}}{3} \ (s \neq t) \tag{8}$$

where E_{ij} is the total multi-hazard exposure susceptibility score of edge ij, g_{ij} is the score under geological hazards, and f_{ij} and e_{ij} are the scores under floods and earthquakes. The score is defined based on exposure susceptibility, as shown in Table 1. Similar to the HDRC strategy, in the ESC strategy, the edges are sequentially removed in descending order based on their ESC. If multiple nodes have the same highest ESC, one of them is chosen at random.

Table 1. Multi-hazard exposure susceptibility score definition.

Score	Very High	High	Medium	Low	Very Low
Geological hazards	5	4	3	2	1
Flood	5	4	3	2	1
Seismic	5	4	3	2	1

3.2.6. The Greedy Algorithm Coefficient

A greedy algorithm is an approach to solving a problem that selects the most appropriate option based on the current situation [35]. In this study, we defined the greedy algorithm coefficient (GAC) based on their associated reliability and robustness metrics. Take the reliability connectivity metric as an example, the GAC for connectivity reliability (GAC-CRel) is calculated as follows:

$$GAC_{ij}^{C\_Rel} = 1 - C\_Rel^{-ij} \tag{9}$$

where $GAC_{ij}^{C\_Rel}$ is the GAC-CRel of edge ij and C_Rel^{-ij} is the connectivity reliability of the highway network after removing edge ij. An edge with a higher $GAC_{ij}^{C\_Rel}$ means that its failure has a great impact on the connectivity reliability of the highway network. For other reliability and robustness metrics, i.e., T_Rel, C_Rob, T_Rob, their GAC-TRel, GAC-CRob, and GAC-TRob, they are calculated as follows:

$$GAC_{ij}^{CT\_R} = 1 - CT\_R^{-ij} \tag{10}$$

where, CT_R are the reliability and robustness metrics, i.e., C_Rel, T_el, C_Rob, T_Rob, and CT_R^{-ij} are the reliability and robustness values after removing edge ij. In the GAC strategy, we sequentially removed the edges in descending order based on their GAC values. If multiple nodes have the same highest GAC, one of them is chosen at random.

4. Results

4.1. Exposure Analysis

Figure 4 and Table 2 show the results of multi-hazard exposure conditions on the highway. According to the results in Table 2, most of the XPCC highways are distributed in areas with a small number of geological hazards (<2) within five kilometers around the highway section, reaching 89.01%. Only 3.69% of the XPCC highways are located in areas with more than ten geological disaster points, mainly distributed in northern Xinjiang. Most of these highways are in XPCC areas 4, 7, 8, and 9. In addition, 7.29% of the XPCC highways are located in areas within range of 2–10 geological disaster points, as shown in Figure 4a,b. Among them, collapses mainly occur on the steep slopes along traffic lines in mountainous areas, near mines, and on natural slopes and cliffs, such as the Tianshan Mountains, Kunlun Mountains, Duku Highway, and China-Pakistan Highway. Landslides are mainly distributed in the piedmont areas, on slopes with loose sediment deposits, such as loess. In Xinjiang, loess-type landslides in the Ili Valley are the most typical. The topographic features of the main debris flow formation areas in Xinjiang are high mountains and deep valleys, the terrain is steep, and the slopes of the mountains are steep. In addition, debris flows in Xinjiang mainly occur in earthquake areas with an intensity of 7 or above on the Richter scale, and the debris flows are accompanied by earthquakes.

Table 2. Multi-hazard exposure information of the XPCC highway.

The Number of Geological Hazard Points	Length/km	Proportion	PGA/g	Length/km	Proportion	Depth/m	Length/km	Proportion
<2	37,661.98	89.01%	≤0.1	19,013.49	44.94%	<0.1	40,476.05	95.66%
2–5	1891.02	4.47%	0.1–0.15	11,270.6	26.64%	0.1–0.2	1019.84	2.41%
5–10	1193.83	2.82%	0.15–0.2	10,158.44	24.01%	0.2–0.4	488.21	1.15%
10–100	1516.24	3.58%	0.2–0.3	1677.77	3.97%	0.4–0.8	222.84	0.53%
≥100	47.8	0.11%	>0.3	190.56	0.45%	0.8–1.8	103.92	0.25%

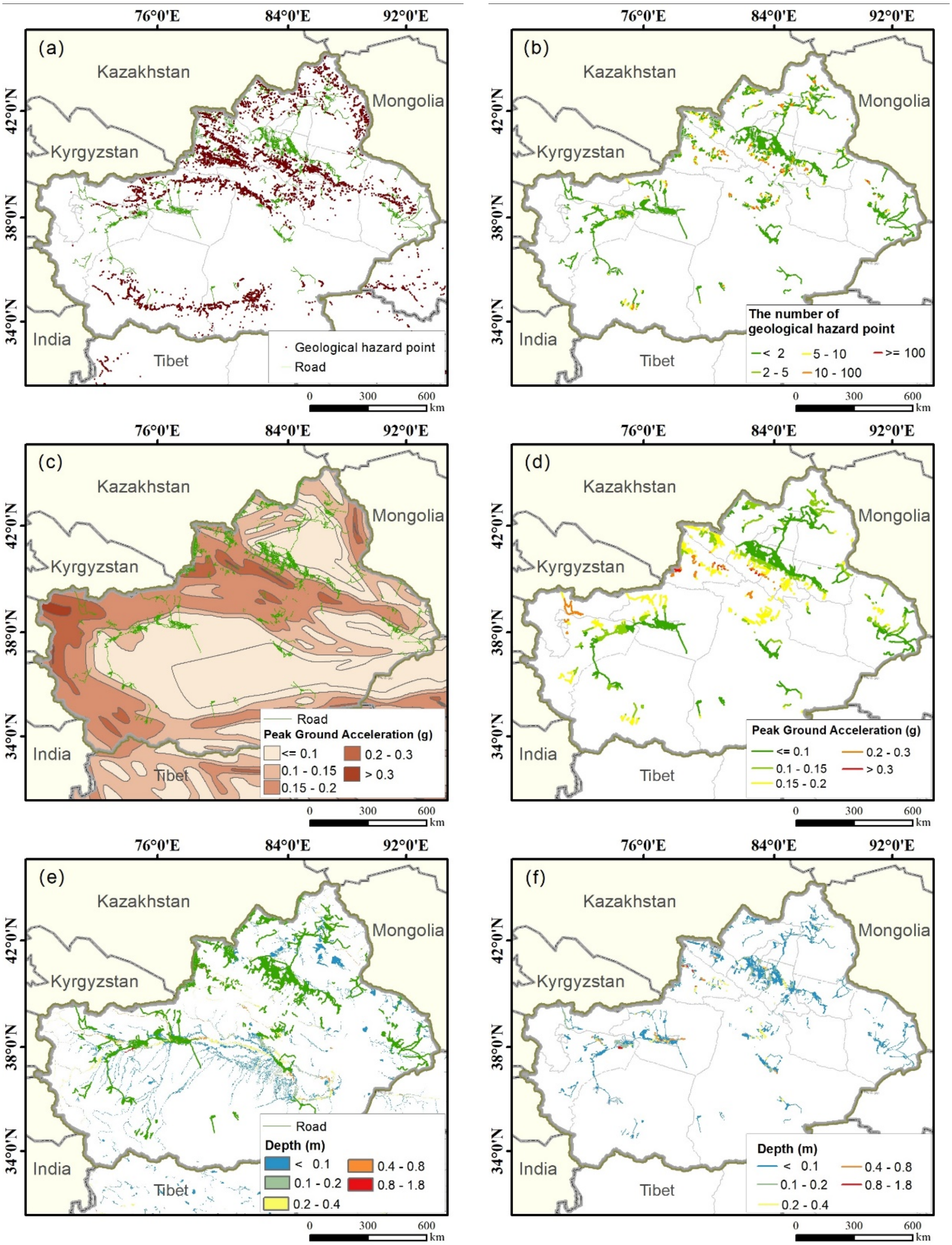

Figure 4. (**a**) The spatial distribution of the geological hazard points, (**b**) geological exposure map of the highway, (**c**) the spatial distribution of earthquakes, (**d**) earthquake exposure map of the highway, (**e**) the spatial distribution of floods, and (**f**) flood exposure map of the highway.

When we look at the earthquake exposure conditions on the highways, we find that most of the XPCC highways are distributed in areas with a low peak ground acceleration ($\leq$0.15 g) occurring once in 475 years, reaching 71.58%. Furthermore, 4.42% of the XPCC highways are located in regions where the ground peak acceleration is greater than 0.2 g. These are mainly distributed in the south Tianshan and north Tianshan seismic zones, primarily in XPCC areas 3, 4, and 8. Additionally, 24.01% of the XPCC highways are located within 0.15–0.2 g of the peak ground acceleration, as shown in Table 2. Xinjiang is an inland area with a high frequency of seismic activity, with high intensity and shallow focus. Quaternary volcanic activity and earthquakes in Xinjiang are strong, and the province is one of the most earthquake-prone provinces in China.

In addition, most of the XPCC highways are distributed in areas with low submerged depth (<0.1 m) of 100-year floods, reaching 95.66%. As seen in Figure 4, the seriously submerged highways are mainly distributed in the flooded areas of the Tarim River, and 0.78% of the highways are located in areas where the flood depth is greater than 0.4 m. These highways are mostly in XPCC areas 1, 3, and 4. In addition, 3.56% of the highways are located within the flood depth of 0.1–0.4 m. Xinjiang's unique landforms lead to floods mainly caused by melting ice and snow. Melting snow floods are the cause of typical highway disasters in northern Xinjiang, and these floods cause serious damage to roadbeds, road surfaces, bridges, and culverts.

4.2. Reliability and Robustness Analysis

Figure 5 shows the spatial distribution of influential edges in the XPCC highway network identified by the HDRC, ESC, GAC-CRel, GAC-TRel, GAC-CRob, and GAC-TRob strategies. The analysis of the HDRC and ESC strategies reveals that the edges with higher rankings are mainly located in the northwest and southwest areas covered by the XPCC, which are more prone to natural hazards. Conversely, the GAC-TRel and GAC-TRob strategies present edges with similar spatial scales, primarily located in the central regions of the highway network, specifically the bridges of nodes. In addition, in the GAC-CRob strategy, edges with higher rankings also tend to be bridges of nodes, but compared with the GAC-TRel and GAC-TRob strategies, they are widespread among the areas covered by the XPCC. Interestingly, the GAC-CRel strategy displays completely different results. Edges with higher rankings are distributed at the end of the highway network, which are the only routes from road-ending nodes to the whole network.

Figure 6 shows the relative reliability and robustness metric changes under different attack strategies for the XPCC arterial highway network. From Figure 6, it can be seen that when the number of removed edges increases, the relative reliability and robustness degradation increases. In addition, the relationship between metrics and edge removal is also different due to the different focuses of each reliability and robustness metric. As seen in Figure 6, the travel time reliability is most affected by four strategies among all of the metrics. The T_Rels are around 0.5 under ESC and GAC-TRel when the number of removed edges reaches 20. When the number of removed edges reaches 100, the T_Rels is decreased to 0.4 under four strategies and is almost close to 0.1 under the GAC-TRel. While the attacks have the most negligible impact on the connectivity reliability, even if the number of removed edges reaches 100, the C_Rel is still greater than 0.7 under all attack strategies. That reveals that network failure brings more significant uncertainty for travel time than connectivity reliability. In addition, connectivity robustness is also easily affected compared to travel time robustness by four strategies.

When comparing the effect between the attack strategies, we find that it is notable that the GAC strategy is the most effective among all strategies for disrupting a network. Limited by the incompleteness of the historical data, the HDRC strategy is similar to a random attack strategy. In contrast, the ESC attack strategy causes greater destruction than the random attack strategy. Take the T_Rob as an example, when the number of removed edges reaches 40, the T_Rob decreases to 65% in the GAC-TRob attack strategy, followed by the ESC attack strategy, for which the value is 80%. The HDRC strategy is similar to a random attack, in which the values are around 90%. When the number of removed edges reaches 80, the T_Rob decreases to 50%. The decreased value is 1.67 times for the ESC attack strategy and 2.5 times for the HDRC and random attack strategies.

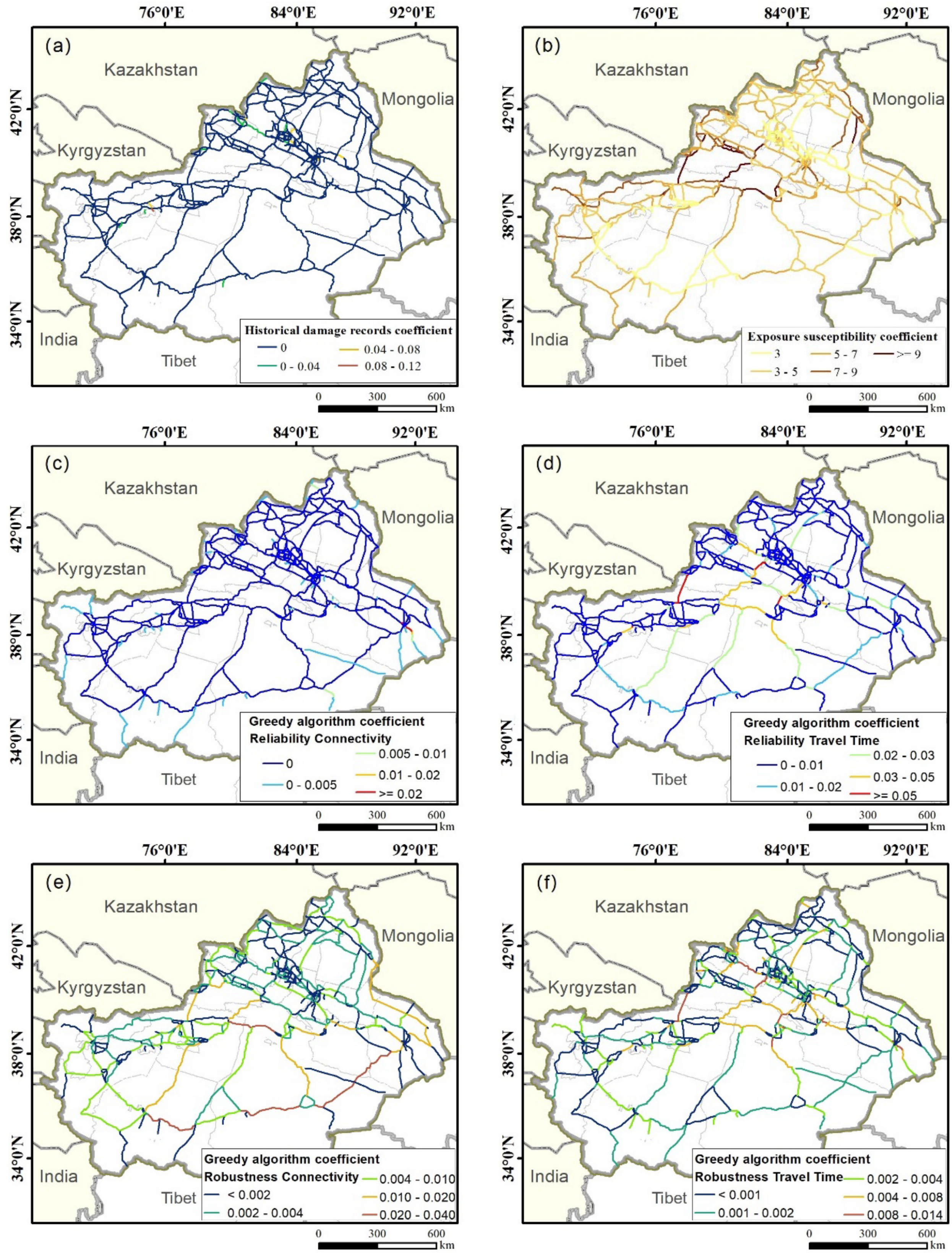

Figure 5. Spatial distribution of the influential edges in the arterial highway network using the (**a**) HDRC, (**b**) ESC, (**c**) GAC-CRel, (**d**) GAC-TRel, (**e**) GAC-CRob, and (**f**) GAC-TRob strategies.

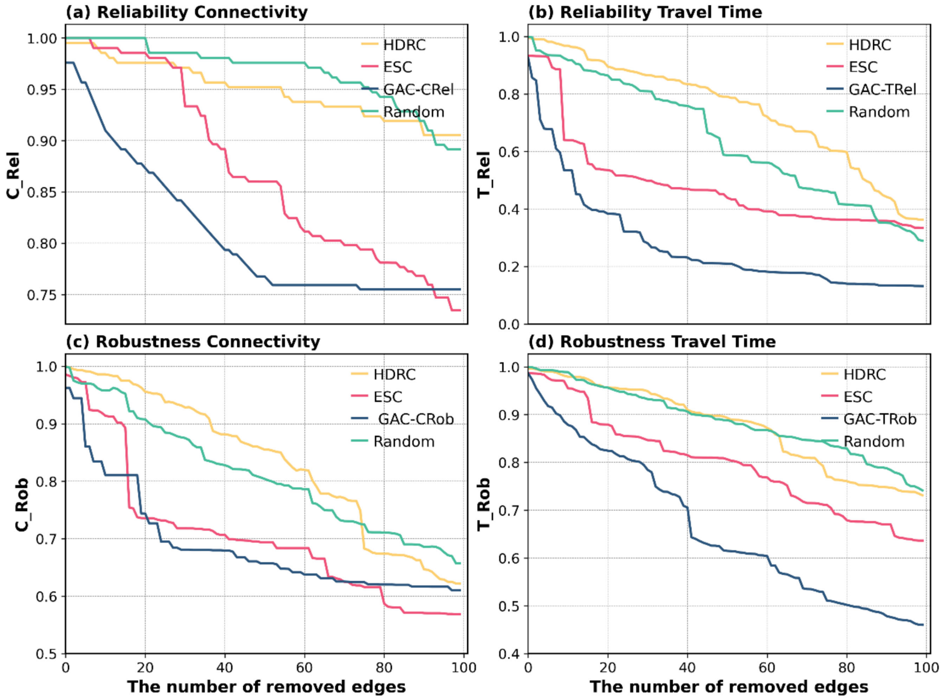

Figure 6. Relative reliability and robustness metrics change for highway network under different attack strategies, (**a**) reliability connectivity, (**b**) reliability travel time, (**c**) robustness connectivity, and (**d**) robustness travel time.

The road network connectivity using Equation (3) and the road network efficiency using Equation (6) for the existing and planned highway networks are given in Table 3, which are the basics for the robustness and reliability assessments. Here, a road with a higher connectivity value demonstrates that information has more chances to transfer, with a higher network efficiency value illustrating that the information transfer is more efficient. For the existing arterial highway network, the road network connectivity is 350,220, which means that every two nodes have 2.099 independent paths to connect. For the planned arterial highway network, the road network connectivity is 505,004, which means that every two nodes have 2.488 independent paths to connect, an 18.56% increase compared to the existing arterial highway network. In addition, the road network efficiency increases from 26,439.18 to 32,288.23, an increase of 22.12% for the planned highway network compared to the existing highway network. When focusing on the average travel time between two nodes, we find that the planned network has not improved much. The average travel time is around 12.4 h, and only 1.08% shorter. This is because most of the new nodes added to the network are located close to the end of the highway network, which can connect remote areas to the city center, but these routes have long travel times.

Table 3. Results of the highway network efficiency and connectivity.

	Road Network Connectivity	Average Independent Paths	Road Network Efficiency	Average Travel Time
The existing arterial highway network	350,220.00	2.10	26,439.18	12.46
The planned arterial highway network	505,004.00	2.50	32,288.23	12.32
The ratio of the change	44.20%	18.56%	22.12%	−1.08%

Figure 7 shows the relative reliability and robustness metrics changes for the planned highway network under different attack strategies. The decreased rules of reliability and robustness in the future highway are the same as in the current situation. The four strategies easily affect the travel time reliability metrics, followed by the travel time robustness metric and connectivity robustness metric. In addition, among all attack strategies, the GAC strategy is the most effective for disrupting a network, followed by the ESC attack strategy. When comparing the reliability and robustness of the existing and planned highway networks, we can see that the connectivity and travel time reliability for the planned highway network are improved under the four attack strategies. In particular, travel time reliability, which is the most easily attacked, is improved by 10% under HDRC and ESC attacks. When focusing on robustness, the connectivity and travel time robustness for the highway network are improved under HDRC, ESC, and random attack strategies in the future while they decrease under some GAC attack scenarios. For example, when the number of removed edges is 18, the connectivity robustness of the planned highway network is 16.84% smaller than in the current situation.

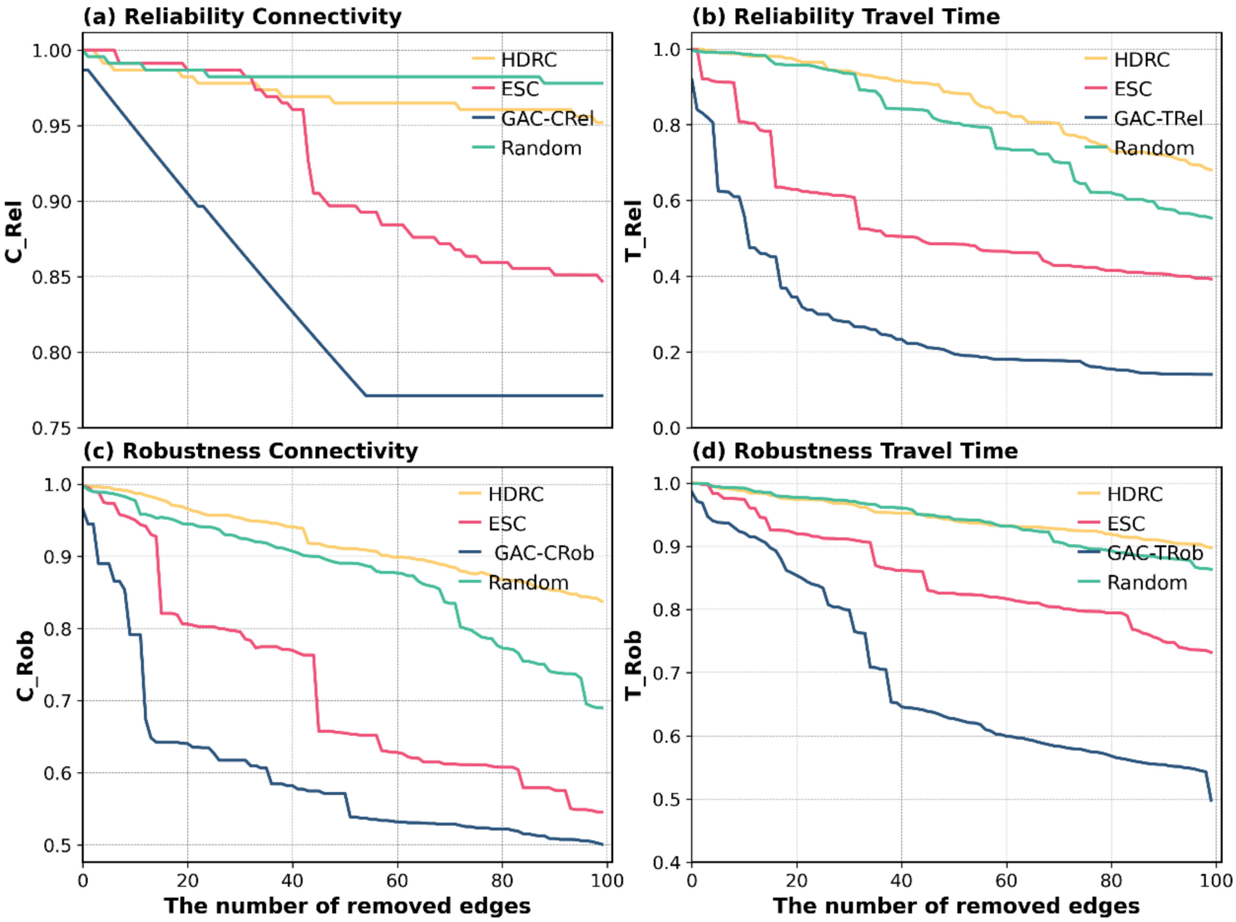

Figure 7. Relative reliability and robustness metrics changes for the planned highway network under different attack strategies, (**a**) reliability connectivity, (**b**) reliability travel time, (**c**) robustness connectivity, and (**d**) robustness travel time.

5. Discussion

In this study, we demonstrated both the most effective attack strategy and the easily affected metrics. Results show that the ESC attack strategy has a higher destruction ability than the random attack strategy, which is close to the GAC strategy. When the number of removed edges reaches 20, the T_Rel decreases to 0.4 under the ESC attack strategy, which means that more than 60% of node pairs need another 10% of the time to be reached. Previous studies have demonstrated that road transportation is critical for post-disaster rescue and recovery [1,2]. The roads connecting people to critical services, such as emergency medical service stations, hospitals, and emergency shelters, are the basis for post-disaster rescue. However, travel time for the rescue roads determined the rescue effectiveness. The terrible thing is that attacks, including multi-hazards, have a negligible impact on connectivity reliability and robustness, while they considerably impact travel time reliability and robustness. The damaged roads will significantly extend the damaging impact on the well-being of communities and the economy because of the lack of timely rescue and freight exchange, as shown in Figure 1.

Several limitations are acknowledged in this analysis. First, with the lack of damage degree information in the historical records, we assume that attacks on highways always have an equivalent effect. In future studies, it would be worth employing reliability and robustness by considering the imbalanced attack capabilities under different scenarios. Second, due to the lack of low-grade highway data, we used the arterial highway network to assess the reliability and robustness, which are not representative of all highways. Since the redundancy for low-grade highways is high, the impact of removing these edges on the reliability and robustness is minor.

6. Conclusions

In this study, we assessed the reliability and robustness of the XPCC arterial highway network based on multi-hazard information. Reliability and robustness metrics are established, considering connectivity and travel time dimensions. We employed four strategies—HDRC, ESC, GAC, and random strategy—to attack the existing and planned XPCC arterial highway network.

The highway network in the northwest and southwest regions covered by the XPCC is highly likely to be affected by multi-hazards because of the complex geological landforms and fragile ecological environments. Meanwhile, the road lines in the center of the highway network and the key bridges of nodes are easily identified as the critical edges under GAC strategies.

Concerning the attack strategies, we found that the ESC attack strategy had a higher destruction capability than the random attack strategy, which was close to the GAC strategy. In addition, attacks had a negligible impact on connectivity reliability and robustness, but they greatly affected travel time reliability and robustness.

The planned arterial highway network has significantly improved the connectivity and efficiency of the highway network by 44.20% in road connectivity and 22.12% in road efficiency compared with the existing highway network. In addition, the planning will improve the reliability and robustness when faced with multi-hazards, especially for travel time reliability. Therefore, governments and transportation bureaus must actively promote resilient transport by increasing redundancy and avoiding disaster-prone areas.

Author Contributions: Data curation, W.Z.; formal analysis, W.Z.; funding acquisition, S.W., S.L. and L.Z.; investigation, X.G. and P.Z.; methodology, W.Z.; project administration, S.W. and S.L.; resources, S.W. and L.Z.; software, W.Z.; supervision, S.W.; validation, W.Z.; visualization, W.Z.; writing–original draft, W.Z.; writing–review and editing, S.W., S.L., X.G., P.Z., L.Z. and W.Z. All authors have read and agreed to the published version of the manuscript.

Funding: This research is financially supported by the Key Science and Technology Project of Transportation Industry (No. 2022-MS1-044) by W.Z. and the Science and Technology Development Project of the Transport Planning and Research Institute, Ministry of Transport (Nos. 092208-214 by W.Z. and 092108-322 by P.Z.).

Institutional Review Board Statement: Not applicable.

Informed Consent Statement: Not applicable.

Data Availability Statement: Not applicable.

Conflicts of Interest: The authors declare no conflict of interest.

References

1. Boakye, J.; Guidotti, R.; Gardoni, P.; Murphy, C. The Role of Transportation Infrastructure on the Impact of Natural Hazards on Communities. *Reliab. Eng. Syst. Saf.* **2022**, *219*, 108184. [CrossRef]
2. Gangwal, U.; Siders, A.R.; Horney, J.; Michael, H.A.; Dong, S. Critical Facility Accessibility and Road Criticality Assessment Considering Flood-Induced Partial Failure. *Sustain. Resilient Infrastruct.* **2023**, *8*, 337–355. [CrossRef]
3. Leslie, J. How Climate Change Is Disrupting the Global Supply Chain. Available online: https://www.preventionweb.net/news/how-climate-change-disrupting-global-supply-chain (accessed on 25 February 2023).
4. Asian Development Bank. People' s Republic of China: Providing Emergency Response to Sichuan Earthquake—Technical Assistance Consultant's Reports. 2008. Available online: https://reliefweb.int/report/china/peoples-republic-china-providing-emergency-response-sichuan-earthquake-technical (accessed on 26 February 2023).
5. Central Committee of the Communist Party of China. National Comprehensive Three-Dimensional Transportation Network Planning Outline. Available online: https://transition-china.org/mobilityposts/policy-briefing-english-translation-national-comprehensive-three-dimensional-transportation-network-planning-outline/ (accessed on 26 February 2023).
6. Nicolosi, V.; Augeri, M.; D'Apuzzo, M.; Evangelisti, A.; Santilli, D. A Probabilistic Approach to the Evaluation of Seismic Resilience in Road Asset Management. *Int. J. Disaster Risk Sci.* **2022**, *13*, 114–124. [CrossRef]
7. Murray-Tuite, P.M. A Comparison of Transportation Network Resilience under Simulated System Optimum and User Equilibrium Conditions. In Proceedings of the 2006 Winter Simulation Conference, Monterey, CA, USA, 3–6 December 2006; pp. 1398–1405. [CrossRef]
8. Zhou, Y.; Wang, J.; Yang, H. Resilience of Transportation Systems: Concepts and Comprehensive Review. *IEEE Trans. Intell. Transp. Syst.* **2019**, *20*, 4262–4276. [CrossRef]
9. Sun, Y.; Xu, R. Rail Transit Travel Time Reliability and Estimation of Passenger Route Choice Behavior. *Transp. Res. Rec.* **2012**, *2275*, 58–67. [CrossRef]
10. Kitamura, S.; Otaka, Y.; Ushizawa, K.; Inoue, S.; Sakata, S.; Kondo, K.; Mukaino, M.; Shimizu, E. Reliability and Validity of the Public Transportation Use Assessment Form for Individuals after Stroke. *Disabil. Rehabil.* **2022**. [CrossRef]
11. Mattsson, L.G.; Jenelius, E. Vulnerability and Resilience of Transport Systems—A Discussion of Recent Research. *Transp. Res. Part A Policy Pract.* **2015**, *81*, 16–34. [CrossRef]
12. Zang, Z.; Xu, X.; Qu, K.; Chen, R.; Chen, A. Travel Time Reliability in Transportation Networks: A Review of Methodological Developments. *Transp. Res. Part C Emerg. Technol.* **2022**, *143*, 103866. [CrossRef]
13. Gu, Y.; Fu, X.; Liu, Z.; Xu, X.; Chen, A. Performance of Transportation Network under Perturbations: Reliability, Vulnerability, and Resilience. *Transp. Res. Part E Logist. Transp. Rev.* **2020**, *133*, 101809. [CrossRef]
14. Jiang, L.; Huang, S. Analyzing Connectivity Reliability and Critical Units for Highway Networks in High-Intensity Seismic Region Using Bayesian Network. *J. Infrastruct. Intell. Resil.* **2022**, *1*, 100006. [CrossRef]
15. Leng, J.Q.; Zhang, Y.P.; Zhang, Q.; Zhao, Y.P. ping Integrated Reliability of Travel Time and Capacity of Urban Road Network under Ice and Snowfall Conditions. *J. Cent. South Univ.* **2010**, *4*, 419–424.
16. Carrion, C.; Levinson, D. Value of Travel Time Reliability: A Review of Current Evidence. *Transp. Res. Part A Policy Pract.* **2012**, *46*, 720–741. [CrossRef]
17. Shams, K.; Asgari, H.; Jin, X. Valuation of Travel Time Reliability in Freight Transportation: A Review and Meta-Analysis of Stated Preference Studies. *Transp. Res. Part A Policy Pract.* **2017**, *102*, 228–243. [CrossRef]
18. De-Los-Santos, A.; Laporte, G.; Mesa, J.A.; Perea, F. Evaluating Passenger Robustness in a Rail Transit Network. *Transp. Res. Part C Emerg. Technol.* **2012**, *20*, 34–46. [CrossRef]
19. Tejedor, A.; Longjas, A.; Zaliapin, I.; Ambroj, S.; Foufoula Georgiou, E. Network Robustness Assessed within a Dual Connectivity Framework: Joint Dynamics of the Active and Idle Networks. *Sci. Rep.* **2017**, *7*, 1–10. [CrossRef]
20. Zhu, W.; Liu, K.; Wang, M.; Yan, X. Enhancing Robustness of Metro Networks Using Strategic Defense. *Phys. A Stat. Mech. its Appl.* **2018**, *503*, 1081–1091. [CrossRef]
21. Bao, Y. The Xinjiang Production and Construction Corps: An Insider's Perspective. *China Int. J.* **2020**, *18*, 161–174.
22. Statistics Bureau of XPCC.2021 National Economic and Social Development Statistical Bulletin of XPCC. Available online: http://epaper.bingtuannet.com/pc/cont/202203/25/c1016621.html (accessed on 26 February 2023).
23. Xinjiang Production and Construction Corps Maintenance Management Center. *Analysis Report on Highway Disaster Damage of the Xinjiang Production and Construction Corps over the Years*; Maintenance Management Center of XPCC: Urumqi, China, 2022.
24. Koks, E.E.; Rozenberg, J.; Zorn, C.; Tariverdi, M.; Vousdoukas, M.; Fraser, S.A.; Hall, J.W.; Hallegatte, S. A Global Multi-Hazard Risk Analysis of Road and Railway Infrastructure Assets. *Nat. Commun.* **2019**, *10*, 2677. [CrossRef]
25. Transport Planning and Research Institute, Ministry of Transport. *Xinjiang Production and Construction Corps Comprehensive Three-Dimensional Transportation Network Planning (2021–2050)*; The Transportation Bureau of XPCC: Urumqi, China, 2022. (In Chinese)
26. Sen, P.; Dasgupta, S.; Chatterjee, A.; Sreeram, P.A.; Mukherjee, G.; Manna, S.S. Small-World Properties of the Indian Railway Network. *Phys. Rev. E Stat. Physics Plasmas Fluids Relat. Interdiscip. Top.* **2003**, *67*, 036106. [CrossRef]
27. Resource and Environment Science and Data Center Spatial Distribution Data of Geological Disaster Points. Available online: https://www.resdc.cn/data.aspx?DATAID=290 (accessed on 1 March 2023).

28. Ward, P.J.; Jongman, B.; Weiland, F.S.; Bouwman, A.; Van Beek, R.; Bierkens, M.F.P.; Ligtvoet, W.; Winsemius, H.C. Assessing Flood Risk at the Global Scale: Model Setup, Results, and Sensitivity. *Environ. Res. Lett.* **2013**, *8*, 044019. [CrossRef]
29. Winsemius, H.C.; Van Beek, L.P.H.; Jongman, B.; Ward, P.J.; Bouwman, A. A Framework for Global River Flood Risk Assessments. *Hydrol. Earth Syst. Sci.* **2013**, *17*, 1871–1892. [CrossRef]
30. Ministry of Transport of People's Republic of China. Technical Standard of Highway Engineering. 2014. Available online: https://www.chinesestandard.net/PDF.aspx/JTGB01-2014 (accessed on 26 February 2023).
31. China Earthquake Administration (CEA). Seismic Ground Motion Parameters Zonation Map of China. 2015. Available online: https://www.gb18306.net/ (accessed on 26 February 2023). (In Chinese)
32. Transport Planning and Research Institute, Ministry of Transport. *Research on Safety Emergency System of XPCC Comprehensive Three-Dimensional Traffic Network in the New Era*; Transport Planning and Research Institute: Beijing, China, 2023. (In Chinese)
33. Newman, M.E.J. Networks: An Introduction. *Astron. Nachrichten* **2010**, *327*, 741–743.
34. Leng, J. *Travel Time Reliability of Urban Road Network under Ice and Snowfall Conditions*; Harbin Institute of Technology: Harbin, China, 2010.
35. Zhang, Z.; Schwartz, S.; Wagner, L.; Miller, W. A Greedy Algorithm for Aligning DNA Sequences. *J. Comput. Biol.* **2000**, *7*, 203–214. [CrossRef]